

Application of TG/FTIR TG/MS and cone calorimetry to understand flame retardancy and catalytic charring mechanism of boron phosphate in flame-retardant PUR–PIR foams

Xiu Liu^{1,2} · Jing-Yu Wang¹ · Xiao-Mei Yang¹ · Yi-Liang Wang¹ · Jian-Wei Hao¹

Received: 4 April 2017 / Accepted: 29 June 2017 / Published online: 10 July 2017
© Akadémiai Kiadó, Budapest, Hungary 2017

Abstract The aim of this work was to investigate the catalysis of boron phosphate (BP) on the thermal stability and char forming in flame-retardant polyurethane–polyisocyanurate foams (FPUR–PIR) with dimethylmethylphosphonate (DMMP) and tris(2-chloropropyl) phosphate (TCPP). The flame-retardant performance and thermal stability of FPUR–PIR were evaluated by cone calorimetry (CONE), thermogravimetric analysis (TG) and microscale combustion calorimetry (MCC). Gas-phase products of FPUR–PIR during the thermal decomposition were investigated via thermogravimetric analyzer coupled with FTIR and mass spectrometry (TG–FTIR–MS). Elemental composition and content of the charred layer in detail were analyzed by X-ray photoelectron spectroscopy (XPS). It was observed that the incorporation of 3 mass% BP in FPUR–PIR decreases the heat release rate, total smoke released and CO production. Meanwhile, the addition of 3 mass% BP advances the release of gaseous products and lower the production of smoke and toxic products like –NCO compounds, PO* and cyanic acid in the gas phase. It can accelerate the dehydration of hydroxyl compounds and promote the char formation of –NCO compounds. This can improve the thermal and oxidation resistance of condensed phase. The catalytic behavior of the dehydration and char formation of BP in the thermal

degradation of FPUR–PIR is attributed to Brønsted and Lewis acidic sites on BP.

Keywords Polyurethane–polyisocyanurate foams · Flame-retardant · Boron phosphate · Catalysis

Introduction

Polyurethane foam is considered to be an ideal alternative to inorganic insulation materials in buildings and insulated appliances [1, 2]. Due to the cell physical structure and chemistry of rigid polyurethane foams, the major disadvantage that prevents them being used as insulation materials especially in buildings is high flammability. Meanwhile, rigid polyurethane foam releases large amount of toxic gases such as carbon monoxide and cyanide in combustion [3].

To improve the flame resistance of rigid polyurethane foams, flame retardants based on halogen, phosphorus, etc. have been used. In particular, some liquid flame retardants such as DMMP and TCPP are widely used due to their excellent flame retardancy, economy and suitability for spraying. However, phosphonate and chlorinated phosphate release abundant phosphorus oxides and volatile combustible organics during combustion [4, 5]. It leads to the further increase in smoke and toxicity production, which is not conducive to fire rescue. As we know, most fire deaths are due to the toxic gases oxygen deprivation and other effects that have been widely referred to as smoke inhalation instead of burns [6]. Smoke and toxicity are very important factors and have been considered in the evaluation of fire safety in new fire safety regulation [7].

Some inorganic compounds as synergistic agents were added in the phosphonates flame-retardant rigid

✉ Jian-Wei Hao
hjw@bit.edu.cn

¹ National Laboratory of Flame Retardant Materials, National Engineering and Technology Research Center of Flame Retardant Materials, School of Materials Science and Engineering, Beijing Institute of Technology, Beijing 100081, China

² Beijing Aerospace Institute of Intelligence and Information, Beijing, China

polyurethane foams to improve the combustion properties and decrease the smoke production [3, 8]. Layered silicates [9, 10], transition metal compounds [11, 12], metal phosphates [13, 14] and metal borates [15, 16], which react by Lewis acid–base interaction or as Friedel–Crafts catalysts, can promote the cross-linking of polymer in some cases. Boron phosphate (BP) was reported due to its environmental friendly and excellent flame-retardant performance. It has been used in polypropylene, polyimide and epoxy as flame retardants or synergistic agents to improve the flame-retardant behaviors. In our previous work, the catalysis action of BP in hydroxyl compounds was investigated. BP has a strong catalysis due to the existence of Brønsted and Lewis acid sites, which can accelerate the dehydration and cross-linking of hydroxyl in compounds [17]. Based on our previous work, we suspect that BP may have a good performance in flame-retardant rigid polyurethane foam, which decomposes to alcohol compounds with large amount of hydroxyl and isocyanate compounds. Not only the catalysis to alcohol compounds but also the charring promotion to isocyanate compounds of BP will be elaborated in this paper.

In this work, BP was used in flame-retardant polyurethane–polyisocyanurate (FPUR–PIR) foams with dimethylmethylphosphonate (DMMP) and tris (2-chloropropyl) phosphate (TCPP). The catalysis flame retardancy and synergy with phosphonate of BP were investigated. This study may provide guidance for the study of BP used in FPUR–PIR foam as synergistic agent to improve the flame retardancy and reduce the smoke and toxic products release in the combustion.

Experimental

Materials

Polyester polyol (4110A, functionality, 3.0; hydroxyl value 410–460 mg KOH g⁻¹; viscosity to 25 °C, 4500 mPa s), polyaryl polymethylene isocyanate (PAPI, NCO%, 30.5; average functionality 2.8; viscosity at 25 °C, 600 mPa s) were all purchased from BASF Co. Ltd. The catalyst employed for cyclotrimerization of isocyanate was 401 (main component is pentamethyldiethylenetriamine), provided by Shanghai Chemical Reagent Co. (Shanghai, China). A silicon-based surfactant NIAx silicon SR-393 as surfactant agent was purchased from Shanghai Chemical Reagent Co. (Shanghai, China). Blowing agent, n-pentane (technical grade) was provided by Shanghai Chemical Reagent Co. of China. Flame retardants, dimethylmethylphosphonate (DMMP) and tris (2-chloropropyl) phosphate (TCPP) were supplied by Jacques Jiangsu Science and Technology Co., Ltd of China. Boron phosphate

(BP) was prepared by the reaction of boric acid and phosphoric acid in laboratory; the mole ratio of element B and P was 1:1, according to the synthesis process elsewhere [18]. The structure is shown in Fig. 1.

Preparation of foams

A one-shot, free rise open method casting method was used to prepare neat PUR–PIR. Test samples with their coats removed were machined in accordance with the test standard. In this study, the molar ratio of NCO to OH was 2.5; the mass ratio of polyol to isocyanate was 100:209. TCPP, DMMP content was fixed at 20 g:10 g per 100 g of polyols; the content of BP is 0, 3, 5 and 8 mass%, respectively.

Characterization

The apparent density of the foam samples was measured according to ASTM D 1622-03, with specimen cut to the dimensions of 30 × 30 × 30 mm³ (length × width × thickness). The apparent densities of five specimens per sample were measured, and then, the average values were reported.

Cone calorimetry (CONE)

CONE measurements were taken at an incident radiant flux of 45 kW m⁻², according to ISO 5660 protocol, using a fire Testing Technology apparatus with a truncated cone-shaped radiator. The specimen (100 × 100 × 30 mm³) was measured horizontally without any grids. Parameters such as heat release rate (HRR), peak heat release rate (PHRR), average specific extinction area (av-SEA), total smoke production (TSP), total smoke released (TSR), total heat released (THR), remaining residue are recorded within the time of 450 s after tests started.

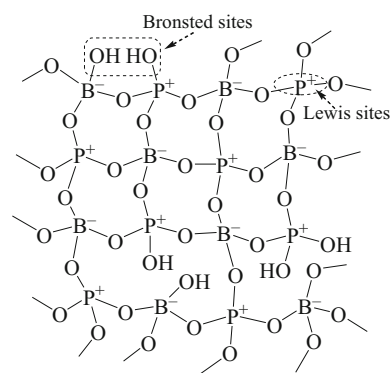


Fig. 1 Structure of boron phosphate [18]

Thermogravimetric (TG)

All TG experiments were performed with 3–5 mg samples in alumina crucibles using a Netzsch 209 F1 thermal analyzer. The measurements were taken in N₂ at a heating rate of 20 °C min⁻¹ from 50 °C to 850 °C.

Microscale combustion calorimetry (MCC)

Pyrolysis combustion experiments were carried out on a Govmark MCC-2 microscale combustion calorimeter. According to the ASTM D 7309-07, about 5 mg of sample was heated to 900 °C at a heating rate of 1 K s⁻¹ and in a stream of nitrogen flowing at 80 cm³ min⁻¹. The reported data are the average of three measurements, and the typical relative error for heat release capacity is ±10%.

Thermogravimetric analysis–Fourier transform infrared–mass spectrometry (TG–FTIR–MS)

The TG–FTIR–MS analysis was performed using Netzsch TG 209 F1 TG instrument coupled with a FTIR (Bruker Tensor 27) and mass spectrometer (Netzsch QMS 403 C). About 10 mg of the sample was heated under helium flow rate of 50 mL min⁻¹ and a heating rate of 10 °C min⁻¹ from 30 to 900 °C. The gas ionization was performed at 100 eV.

Scanning electron microscopy (SEM)

The surfaces of the samples after CONE test were observed with an S-4800 (JEOL Japan) SEM with an accelerating voltage of 5 kV.

X-ray photoelectron spectroscopy (XPS)

XPS spectra (Al K α) of solid residues were recorded on a PHI Quantera-II SXM (Ulvac-PHI, Inc.) at 25 W under a vacuum of 2.6×10^{-7} Pa. The spectrometer was calibrated using the binding energy of adventitious carbon as 284.8 eV.

Results and discussion

Combustion behaviors

The formulas and the density of various PUR–PIR systems are listed in Table 1. In this work, flame-retardant content is 10 mass%, and various contents of BP 1, 3, 5 and 8 mass% are incorporated in the flame-retardant PUR–PIR with TCPP and DMMP. The density of various formula foams is about 42 ± 2 kg m⁻³.

Table 1 Sample code, composition and density of PUR–PIR, FPUR–PIR and BP incorporated FPUR–PIR

| Sample | PUR–PIR | FR | BP | Density/kg m ⁻³ |
|--------------|---------|----|----|----------------------------|
| PUR–PIR | 100 | 0 | 0 | 43.7 |
| FPUR–PIR | 100 | 10 | 0 | 39.2 |
| FPUR–PIR–BP1 | 100 | 10 | 1 | 40.5 |
| FPUR–PIR–BP3 | 100 | 10 | 3 | 40.7 |
| FPUR–PIR–BP5 | 100 | 10 | 5 | 42.5 |
| FPUR–PIR–BP8 | 100 | 10 | 8 | 43.3 |

Cone calorimeter that based on the oxygen consumption principle was used to investigate the combustion behaviors of materials. Some important informations such as heat release rate (HRR), total smoke released (TSR), CO production (COP), peak of heat released rate (PHRR), total heat release (THR), average specific extinction area (av-SEA), total smoke production (TSP) and residual mass are provided in Fig. 2 and Table 2. The addition of 10 mass% flame retardants decreases the HRR about 10%, but increases the TSR about 13.3% compare with pure PUR–PIR. It is as a result of the gas-phase flame retardancy effect of phosphonate, which released phosphonate fragments in gas phase to capture free radicals during the combustion [19]. The incorporation of 1, 3 mass% BP in FPUR–PIR decreases the HRR, TSR and COP. However, as the amount of BP is over 3 mass%, the combustion properties were deteriorated, the smoke production was increased dramatically. In the formula with 8 mass% BP, we can see the thermal degradation is accelerated and two thermal degradation peaks are very close. It means that sample degrades rapidly and releases large amount of degradation fragments in short time. Meanwhile, pure char residue of samples incorporated BP decreases with the increase in BP loading. It may be interpreted that BP has a strong catalyst action during the combustion. Under lower amount, it has synergy with phosphonate flame retardant and improves the flame-retardant behaviors. But large amount of BP would deteriorate the flame-retardant behaviors by the strong acid catalyst action, which can speed up the thermal degradation of FPUR–PIR and make the decomposition fragments have no time to cross-link and interact.

Thermal stability

TG analysis

The mass loss behavior was analyzed by TG for exploring the basic degradation information. The TG curves of all the samples at 20 °C min⁻¹ under nitrogen atmosphere are shown in Fig. 3. The detailed data such as mass loss rate at

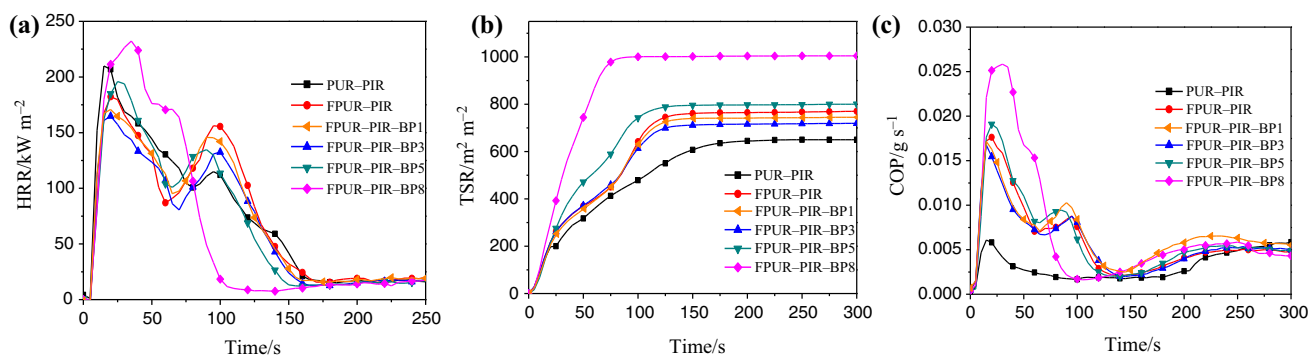


Fig. 2 **a** HRR, **b** TSR and **c** COP curves of PUR-PIR, FPUR-PIR and FPUR-PIR with BP (45 kW m^{-2})

Table 2 Cone calorimetric data of PUR-PIR, FPUR-PIR and FPUR-PIR filled with BP (heat flux of 45 kW m^{-2})

| Sample | pk-HRR/ kW m^{-2} | THR/ MJ m^{-2} | TSP/ $\text{m}^2 \text{ kg}^{-1}$ | av-SEA/ $\text{m}^2 \text{ kg}^{-1}$ | Residual mass/% | Pure char residue/% ^a |
|--------------|----------------------------|-------------------------|-----------------------------------|--------------------------------------|-----------------|----------------------------------|
| PUR-PIR | 209.8 ± 3.9 | 31.5 ± 0.8 | 6.0 ± 0.3 | 537.3 ± 21 | 20.6 | 20.6 |
| FPUR-PIR | 182.3 ± 2.6 | 21.3 ± 0.4 | 6.8 ± 0.2 | 734.2 ± 15 | 18.8 | 18.8 |
| FPUR-PIR-BP1 | 174.2 ± 1.2 | 20.7 ± 0.4 | 6.6 ± 0.3 | 693.3 ± 16 | 22.7 | 21.7 |
| FPUR-PIR-BP3 | 164.9 ± 4.2 | 19.2 ± 1.0 | 6.4 ± 0.1 | 643.2 ± 12 | 27.3 | 24.3 |
| FPUR-PIR-BP5 | 189.9 ± 1.3 | 19.4 ± 0.3 | 7.1 ± 0.5 | 698.9 ± 7 | 28.2 | 23.2 |
| FPUR-PIR-BP8 | 232.4 ± 0.8 | 20.4 ± 0.2 | 8.9 ± 0.2 | 823.5 ± 9 | 29.1 | 21.1 |

^a Amount of the purified char (the amount of BP is subtracted from the residue) divided by the amount of sample

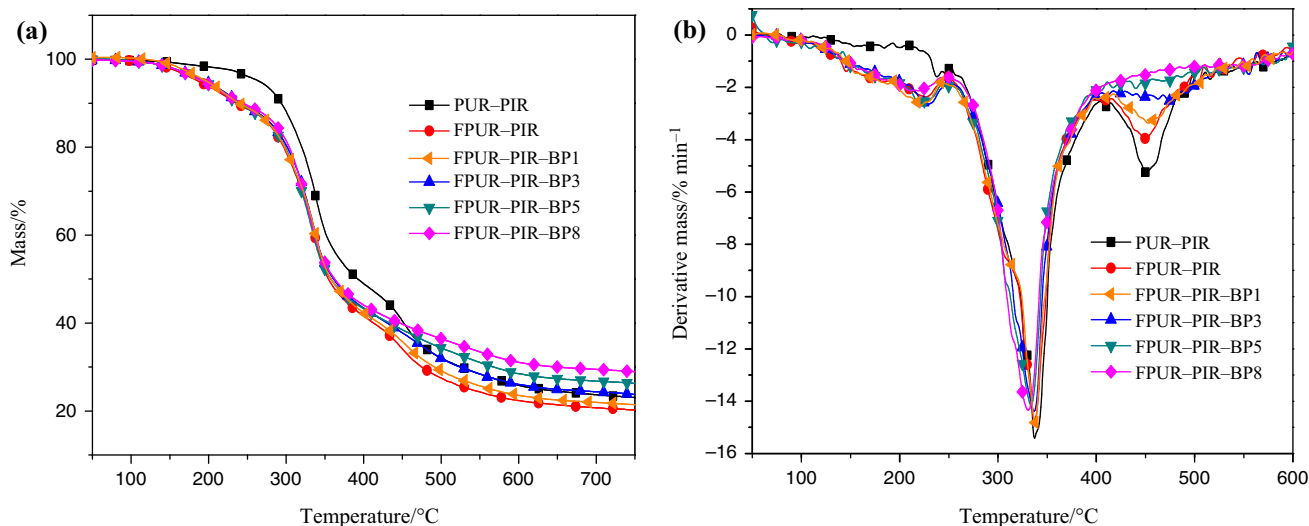


Fig. 3 **a** TG and **b** DTG curves of PUR-PIR, FPUR-PIR and FPUR-PIR filled with BP under nitrogen

the thermal degradation peaks and char yields at $750 \text{ }^\circ\text{C}$ are listed in Table 3. As shown in Fig. 3 and Table 3, the neat PUR-PIR shows three-step mass loss. The first stage at $200\text{--}280 \text{ }^\circ\text{C}$ is due to the volatilization of phosphonate and other small molecule compounds, whereas the second can be ascribed to the pyrolysis of the PUR-PIR at around $340 \text{ }^\circ\text{C}$ and the third stage is attributed to the further decomposition of char layer when the temperature is higher than $430 \text{ }^\circ\text{C}$.

As for the degradation of neat PUR-PIR, the first degradation peak is not obvious. The addition of phosphonate flame retardants increased the mass loss rate of first peak from 1.5 to $2.4 \text{ } \text{min}^{-1}$. The incorporation of various amounts of BP, the mass loss rates of first decomposition peak were increased and the mass loss rates of second decomposition peak were decreased compared with FPUR-PIR. It is worth noting that the third decomposition peaks were disappeared with the addition of more

Table 3 TG data of PUR-PIR, FPUR-PIR and FPUR-PIR filled with BP under nitrogen

| Sample | First peak | | Second peak | | Third peak | | Char residue at 750 °C/% | Pure char residue at 750 °C/% ^a |
|--------------|------------|------------------------------------|-------------|------------------------------------|------------|------------------------------------|--------------------------|--|
| | Temp/°C | Mass loss rate/% min ⁻¹ | Temp/°C | Mass loss rate/% min ⁻¹ | Temp/°C | Mass loss rate/% min ⁻¹ | | |
| PUR-PIR | 238.4 | 1.5 | 338.3 | 15.2 | 451.2 | 5.2 | 23.1 | 23.1 |
| FPUR-PIR | 226.5 | 2.4 | 337.1 | 14.7 | 450.4 | 4.0 | 18.1 | 18.1 |
| FPUR-PIR-BP1 | 226.7 | 2.5 | 337.1 | 14.8 | 458.2 | 3.7 | 21.2 | 20.2 |
| FPUR-PIR-BP3 | 228.0 | 2.7 | 336.8 | 14.4 | 474.3 | 2.5 | 23.8 | 20.8 |
| FPUR-PIR-BP5 | 220.1 | 2.7 | 333.5 | 14.2 | – | – | 26.3 | 21.3 |
| FPUR-PIR-BP8 | 218.9 | 2.6 | 330.7 | 14.3 | – | – | 29.5 | 21.5 |

^a Amount of the purified char (the amount of BP is subtracted from the residue) divided by the amount of sample

than 3 mass% BP. As listed in Table 3, the char yields of the FPUR-PIR filled with BP were significantly increased from 18.1 to 29.5% with 8 mass% BP. From the pure char residue, we can see the results are different with CONE test, which is due to different sample scales and test environment of TG and cone calorimeter. It indicated that BP and FPUR-PIR matrix have some chemical reactions. It may be attributed to that BP can catalyze the thermal degradation at the initial stage, then promote the char forming and keep more thermal degradation fragments in condensed phase which result in the decrease in mass loss.

MCC test

MCC is a new and useful method developed by Lyon and Walters, which was used to determine on a milligram scale, and it has many advantages on evaluation of polymer decomposition in comparison with other conventional large-scale calorimetry methods [20]. The heat release rate (HRR) curves and detailed MCC data such as the peak heat release rate (PHRR) and the total heat release (THR) are presented in

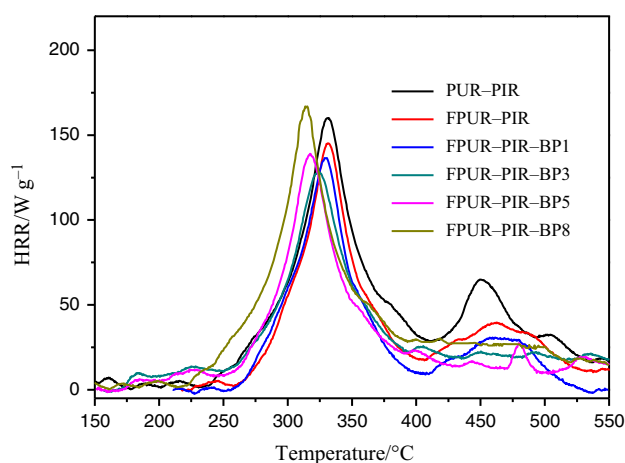


Fig. 4 HRR of PUR-PIR, FPUR-PIR and FPUR-PIR-BP from MCC

Table 4 Detailed data of PUR-PIR, FPUR-PIR and FPUR-PIR filled with BP from MCC

| Sample | Peak HRR/W g ⁻¹ | THR/kJ g ⁻¹ | Residue/%, 850 °C |
|--------------|----------------------------|------------------------|-------------------|
| PUR-PIR | 160.2 | 18.7 | 21.7 |
| FPUR-PIR | 140.7 | 11.6 | 18.5 |
| FPUR-PIR-BP1 | 138.6 | 12.0 | 22.0 |
| FPUR-PIR-BP3 | 126.6 | 10.5 | 23.1 |
| FPUR-PIR-BP5 | 138.2 | 11.8 | 25.4 |
| FPUR-PIR-BP8 | 160.5 | 12.4 | 28.3 |

Fig. 4 and Table 4. The addition of 10 mass% phosphonate flame retardants decreases the HRR and THR of PUR-PIR. The incorporation of 3 mass% BP further decreases the HRR and THR of FPUR-PIR. However, the HRR was increased about 14.3% when the amount of BP is 8 mass%. Furthermore, BP alters the thermal degradation stages of FPUR-PIR. Pure PUR-PIR has two obvious thermal degradation peaks, FPUR-PIR has a small degradation peak at 420–450 °C, but it hardly to find the peak for FPUR-PIR incorporated BP. In addition, BP increases the char residue value at 850 °C. This may be due to the char-forming action of BP, which promote the cross-linking of thermal degradation fragments and keep it in the condensed phase. MCC results are not entirely fit with the CONE results due to different sample scales and test environment. Different with CONE test, MCC separately reproduces the solid state and gas phase of combustion by controlled pyrolysis of the sample in an inert gas stream followed by high-temperature oxidation of volatile pyrolysis products. So the combustion of sample in MCC test is more complete. The char residue value for the same sample in MCC test is lower than in CONE test.

TG-FTIR-MS analysis

Based on the interpretation of CONE, TG and MCC data, FPUR-PIR filled with 3 mass% BP has a lower smoke

production and shows excellent char formation compared to other formulas. To understand the catalysis of BP in FPUR-PIR, additional investigations into FPUR-PIR filled with 3 mass% BP were carried out. The TG-FTIR-MS technique can give information about the pyrolysis products, which provides insight into the thermal degradation mechanisms. In order to analyze the influence of BP in gas phase of FPUR-PIR during the thermal degradation, TG-FTIR-MS was utilized to identify the gas products.

The gaseous products of FPUR-PIR and FPUR-PIR with BP at different temperatures during the degradation process are shown in Fig. 5. Peaks in the regions of about 900–1300, 1500–1800, 2200–2500, 2800–3000 and 3500–3700 cm^{-1} which assigned to NH_3 , phosphorus compounds, -NCO compounds, CO_2 , hydrocarbons and water are highly noted [21]. As Fig. 5 illustrates, the addition of 3 mass% BP increases the CO_2 production of FPUR-PIR at 324 °C with the same sample mass. It may be attributed to that BP accelerates and advances the decomposition of FPUR-PIR at the initial stage.

To further understand the effects of additives on evolved gases, the relation between relative intensity of characteristic peak and time for evolved CO_2 , -NCO compounds, PO^* and hydroxyl compounds under the same sample mass is shown in Fig. 6. It can be seen that the addition of BP advances the release of gaseous products and lower the production of CO_2 , -NCO compounds, PO^* and hydroxyl compounds. The release peak of -NCO compounds is at about 1800 s corresponded to 320–350 °C which already reported in studies [22, 23]. The reduction of NH_3 and -NCO compounds can decrease the toxicity of the gaseous products from FPUR-PIR. The phosphorus compounds release early than other gaseous products due to the low

thermal degradation temperature of phosphonate flame retardants. BP reduces the production of PO^* , especially decrease the release peak at about 2000 s. In addition, the production of hydroxyl compound was decreased. It is because BP has a lot of Brønsted and Lewis acid sites on the surface, which can accelerate the decomposition of FPUR-PIR and promote the cross-linking of hydroxyl compounds [17], -NCO compounds and other fragments to keep more phosphorus oxides, nitrogen compounds and decomposition fragments in the condensed phase.

Meanwhile, the evolved products during the thermal degradation of FPUR-PIR and FPUR-PIR-BP3 were determined by TG-MS and are illustrated in Fig. 7. The intensity curves of water (m/z 18), cyanic acid (m/z 43), CO_2 (m/z 44) and C-4 butylene (m/z 56) [24, 25] with time are shown. It can be seen FPUR-PIR-BP3 degrades earlier than FPUR-PIR, which is consistent with TG-FTIR results. With the same sample mass, FPUR-PIR-BP3 has the lower intensity in water, cyanic acid, CO_2 and C-4 butylene. As we know, the cyanic acid is a toxic compound, which can lead to the lung injured [26], and C-4 butylene is the precursor of smoke [27]. It means that the addition of BP lowers the smoke and toxicity action in the gas phase. It is probably induced by the Brønsted and Lewis acid catalysis of BP in the combustion, which can catalyze the decomposition of FPUR-PIR and promote the cross-linking of decomposition fragments to form char layer. Firstly, BP promotes the dehydration of hydroxyl which release from the decomposition of polyurethane foam and form the unsaturation bonds. Then, the unsaturation bonds and decomposition fragments such as -NCO compounds cross-link each other and keep in condensed phase to form char layer, which is consistent with the results of previous study [17].

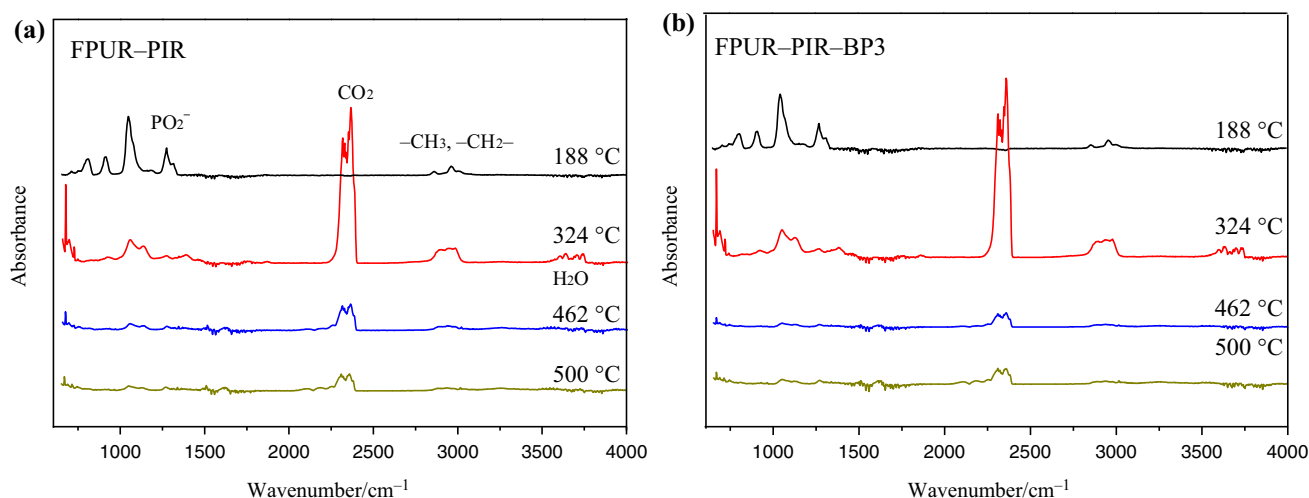


Fig. 5 FTIR spectra of **a** FPUR-PIR, **b** FPUR-PIR-BP3 evolved gases at different temperatures in helium

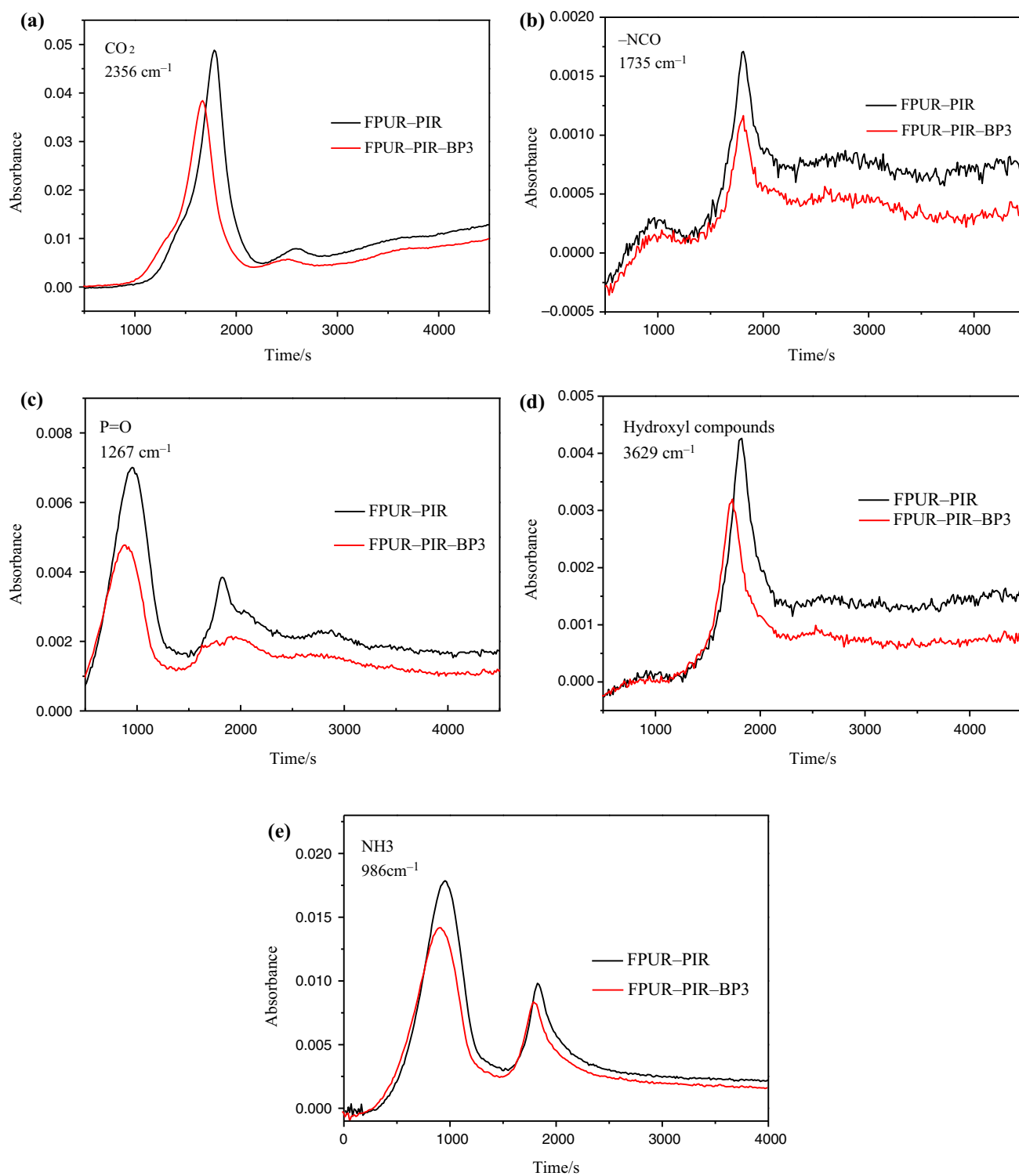


Fig. 6 Comparison of TG-FTIR spectra of pyrolysis products for FPUR-PIR and FPUR-PIR-BP3

Char residue

To further understand the condensed phase activity of the flame retardants, the residues of FPUR-PIR after CONE test were characterized using SEM. As shown in Figs. 8

and 9, the char of pure PUR-PIR shows a loose structure, which indicates inefficient barrier protection for underlying layers. Compared to the char of PUR-PIR, the char of FPUR-PIR is coherent, but still has some cracks on the surface. After the addition of BP, the char

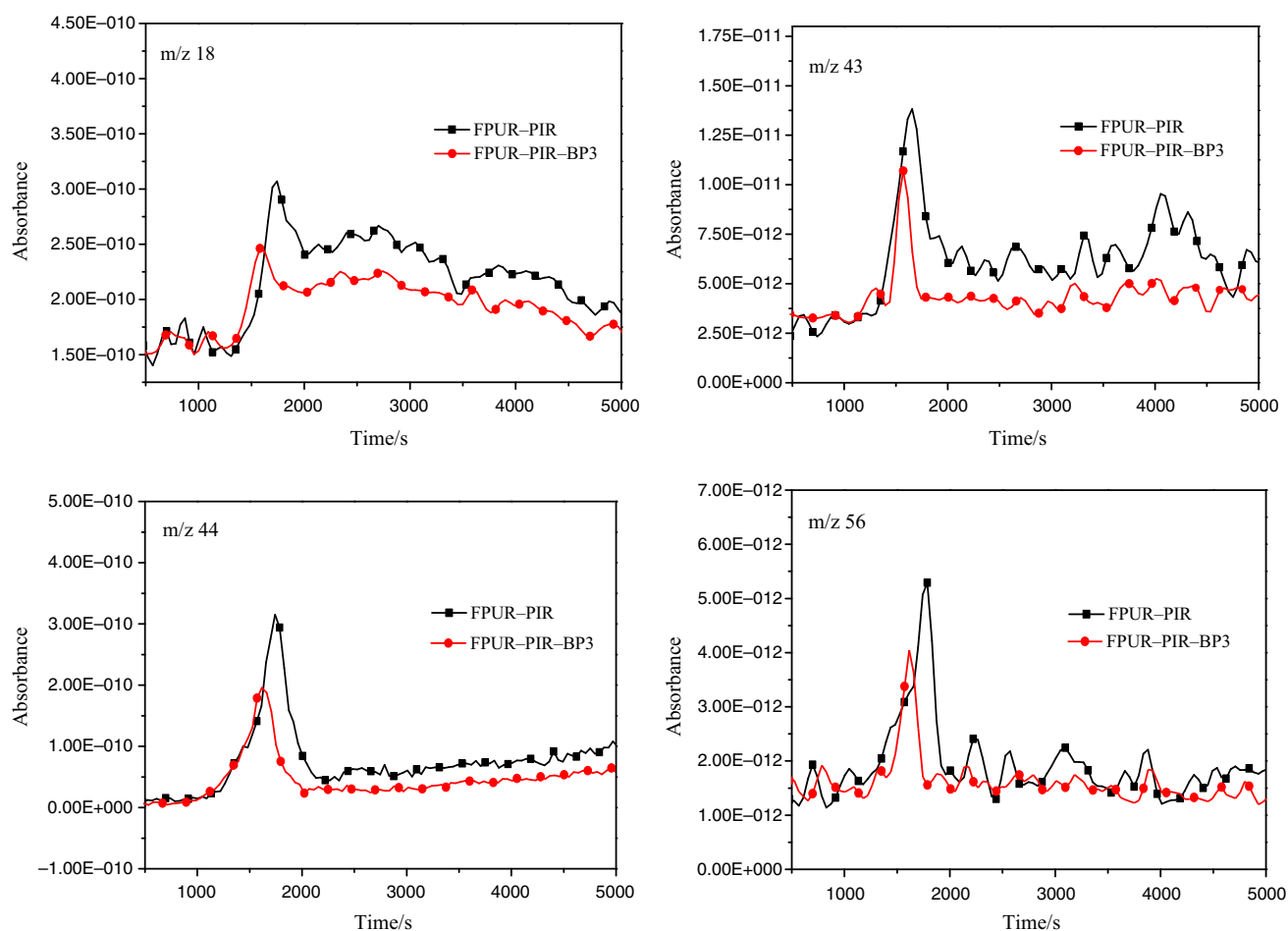


Fig. 7 Comparison of TG-MS spectra of pyrolysis products for FPUR-PIR and FPUR-PIR-BP3

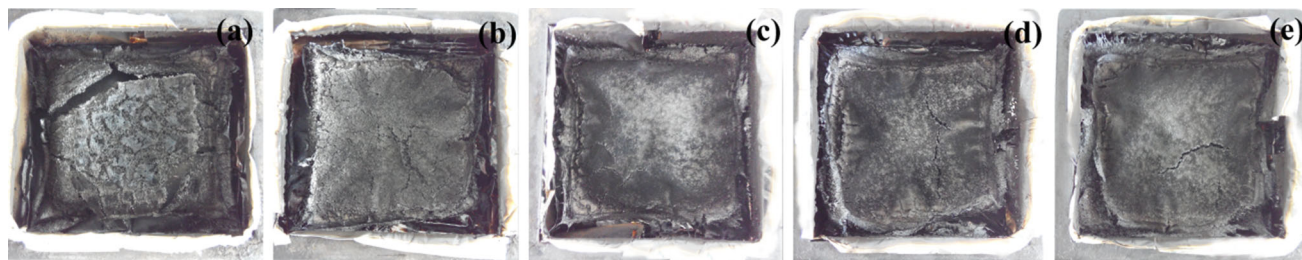


Fig. 8 Digital photographs of residue char after CONE test a PUR-PIR, b FPUR-PIR, c FPUR-PIR-BP3, d FPUR-PIR-BP5, e FPUR-PIR-BP8

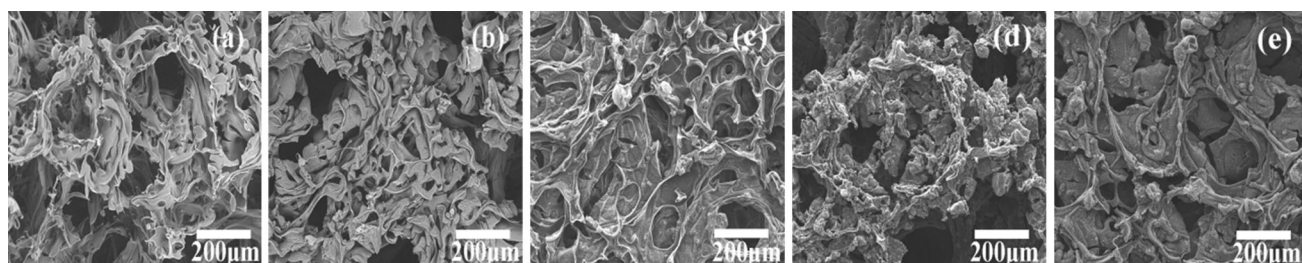


Fig. 9 SEM images of the char residues after CONE test a PUR-PIR, b FPUR-PIR, c FPUR-PIR-BP3, d FPUR-PIR-BP5, e FPUR-PIR-BP8

Table 5 Comparison of atomic ratios of FPUR–PIR and FPUR–PIR–BP3 residues in CONE test

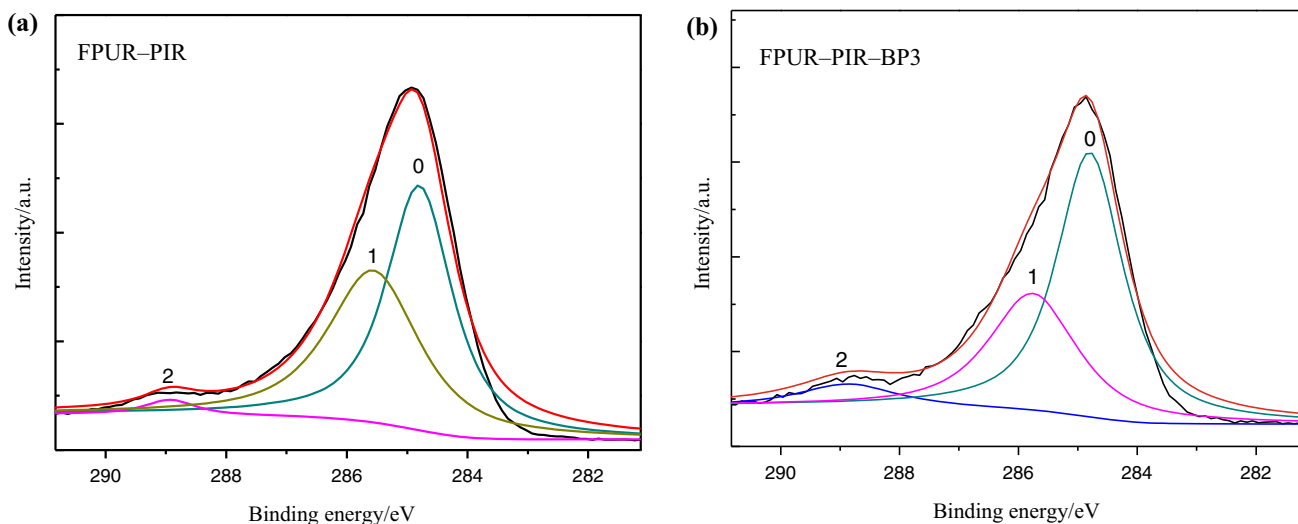
| Sample | Mole content/mol% | | | | | Atomic ratio of C/O |
|--------------|-------------------|-----|------|-----|------|---------------------|
| | C | N | O | P | B | |
| FPUR–PIR | 77.7 | 7.5 | 14.1 | 0.7 | – | 5.5 |
| FPUR–PIR–BP3 | 50.7 | 4.0 | 25.2 | 4.7 | 15.4 | 2.0 |

structures are more continuous and compact. Especially the FPUR–PIR filled with 3 mass% BP, we can see some black char on the surface which can improve the strength of char layer.

XPS provides information about elemental composition and content of the charred layer in detail. The char residues of FPUR–PIR and FPUR–PIR–BP3 after CONE test were analyzed by XPS. The contents of several elements present in charred layers obtained from FPUR–PIR and FPUR–PIR–BP3 are listed in Table 5. The incorporation of BP increases the phosphorus content. The atomic ratio of C/O was decreased from 5.5 to 2.0. It means more oxygen elements are kept in the condensed phase. C1s spectrums in Fig. 10 were deconvoluted into three components with fixed positions adopted in the analysis of the C1s region of

carbon materials. The different binding energies (BE) of carbon were provided. The components in Table 6 represent graphitic carbon C–C and C=C (peak 0, BE = 284.8 eV), aliphatic carbon (peak 1, BE = 285.6 eV), carbon in thermal oxidation products such as COOH and –C(O)–O–C (peak 2, BE = 288.9 eV). As the data show, the incorporation of 3 mass% BP, the content of C–C and C=C (peak 0) increases from 52.5 to 58.4%. C–C and C=C are thermal stability structures in the char layer, which can increase the thermal and oxidation resistance of condensed phase.

In Fig. 11, N1s spectrums were deconvoluted into two components. The peaks at 400.0 eV and 398.3 eV can be attributed to C=N and C–N, respectively [27, 28]. It was found out that the addition of 3 mass% BP increased the content of C=N in char residues from 54.2 to 68.3% (Table 7). The carbon and nitrogen conjugated bond is probably came from the interaction of thermal degradation fragments. It may be attributed to some stable structures such as carbodiimide, which can be formed by the interaction of –NCO groups and alcohol compounds during the thermal degradation of polyurethane [29]. The results indicate that BP catalyzes the transformation of –NCO groups to thermal stable structures and promotes the

**Fig. 10** C1s spectra of the char residues of **a** FPUR–PIR and **b** FPUR–PIR–BP3**Table 6** C1s curve fitting of FPUR–PIR and FPUR–PIR–BP3 residues in CONE test

| Peak | FPUR–PIR | | | FPUR–PIR–BP3 | | | Assignment |
|------|-------------|----------|------|--------------|----------|------|-----------------|
| | Position/eV | Area/CPS | A/% | Position/eV | Area/CPS | A/% | |
| 0 | 284.8 | 21,535.4 | 52.5 | 284.8 | 13,700.5 | 58.4 | C–C, C=C |
| 1 | 285.6 | 18,522.0 | 45.1 | 285.7 | 8030.5 | 34.3 | Aliphatic |
| 2 | 288.9 | 1000.0 | 2.4 | 288.9 | 1709.8 | 7.3 | COOH, –C(O)–O–C |

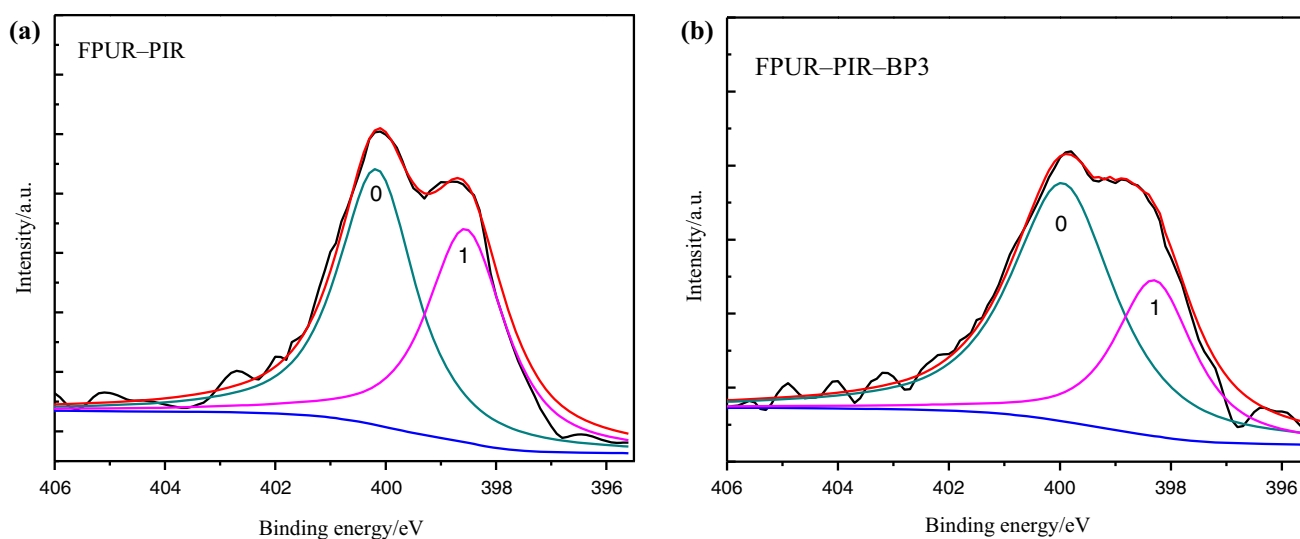


Fig. 11 N1s spectra of the char residues of **a** FPUR-PIR and **b** FPUR-PIR-BP3

Table 7 N1s curve fitting of FPUR-PIR and FPUR-PIR-BP3 residues in CONE test

| Peak | FPUR-PIR | | | FPUR-PIR-BP3 | | | Assignment |
|------|-------------|----------|------|--------------|----------|------|------------|
| | Position/eV | Area/CPS | A/% | Position/eV | Area/CPS | A/% | |
| 0 | 400.1 | 2107.9 | 54.2 | 399.8 | 2080.3 | 68.3 | C=N |
| 1 | 398.4 | 1783.4 | 45.8 | 398.3 | 1051.8 | 31.7 | C-N |

formation of C=N groups in condensed phase. It performs the cross-linking and formation of char layer and keeps more degradation fragments in condensed phase, which increase the stability of char residue and decrease the smoke and toxicant production.

Conclusions

In this paper, the acid catalysis of BP in flame-retardant PUR-PIR with dimethylmethylphosphonate (DMMP) and tris (2-chloropropyl) phosphate (TCPP) was investigated. It was noted from the CONE data that the incorporation of 3 mass% BP in FPUR-PIR decreases the HRR, TSR and COP. However, as the amount of BP is over 3 mass%, the combustion properties were deteriorated, and the smoke production was increased dramatically. TG and MCC results showed that BP accelerates the thermal degradation of FPUR-PIR and increases the amount of char yield. According to the characterization of TG-FTIR-MS, the addition of BP in FPUR-PIR lowers the production of smoke and toxicity gases during the thermal degradation. Meanwhile, BP promoted the interaction and cross-linking of hydroxyl compounds and catalyzed the transformation of -NCO to stable structures in condensed phase and

retained more decomposition products in the solid phase. It is induced by the Brønsted and Lewis acid catalysis of BP in the combustion. The catalysis and char-forming effect of BP in FPUR-PIR were elaborated.

Acknowledgements The work was financially supported by National Natural Science Foundation of China (No. 21474008) and National Key R&D Program of China (No. 2016YFB0302104).

References

- Ciecierska E, Jurczyk-Kowalska M, Bazarnik P, Kowalski M, Krauze S, Lewandowska M. The influence of carbon fillers on the thermal properties of polyurethane foam. *J Therm Anal Calorim.* 2016;123(1):283–91. doi:10.1007/s10973-015-4940-2.
- Yang R, Hu W, Xu L, Song Y, Li J. Synthesis, mechanical properties and fire behaviors of rigid polyurethane foam with a reactive flame retardant containing phosphazene and phosphate. *Polym Degrad Stabil.* 2015;122:102–9. doi:10.1016/j.polydegradstab.2015.10.007.
- Liu X, Xu DM, Wang YL, Zhou Y, Hao JW. Smoke and toxicity suppression properties of ferrites on flame-retardant polyurethane-polyisocyanurate foams filled with phosphonate. *J Therm Anal Calorim.* 2016;. doi:10.1007/s10973-016-5356-3.
- Gaan S, Liang SY, Mispereuve H, Perler H, Naescher R, Neisius M. Flame retardant flexible polyurethane foams from novel DOPO-phosphonamidate additives. *Polym Degrad Stabil.* 2015;113:180–8. doi:10.1016/j.polydegradstab.2015.01.007.

5. Liang S, Neisius M, Mispreve H, Naescher R, Gaan S. Flame retardancy and thermal decomposition of flexible polyurethane foams: structural influence of organophosphorus compounds. *Polym Degrad Stabil.* 2012;97(11):2428–40. doi:10.1016/j.polydegradstab.2012.07.019.
6. Jiao CM, Zhang CJ, Dong J, Chen XL, Qian Y, Li SX. Combustion behavior and thermal pyrolysis kinetics of flame-retardant epoxy composites based on organic-inorganic intumescent flame retardant. *J Therm Anal Calorim.* 2015;119(3):1759–67. doi:10.1007/s10973-014-4379-x.
7. Final Draft prEN 13501-1: Fire classification of construction products and building elements. Part 1: classification using test data from reaction to fire tests; 2007.
8. Liu X, Zhou Y, Hao JW, Du JX. Smoke and toxicity suppression by zinc salts in flame-retardant polyurethane-polyisocyanurate foams filled with phosphonate and chlorinated phosphate. *J Appl Polym Sci.* 2015;132(16):41846. doi:10.1002/app.41846.
9. Bellucci F, Camino G, Frache A, Saffa A. Catalytic charring-volatilization competition in organoclay nanocomposites. *Polym Degrad Stabil.* 2007;92(3):425–36. doi:10.1016/j.polydegradstab.2006.11.006.
10. Zheng XR, Wang GJ, Xu W. Roles of organically-modified montmorillonite and phosphorous flame retardant during the combustion of rigid polyurethane foam. *Polym Degrad Stabil.* 2014;101:32–9. doi:10.1016/j.polydegradstab.2014.01.015.
11. Holdsworth AF, Horrocks AR, Kandola BK, Price D. The potential of metal oxalates as novel flame retardants and synergists for engineering polymers. *Polym Degrad Stabil.* 2014;110:290–7. doi:10.1016/j.polydegradstab.2014.09.007.
12. Lewin M, Endo M. Catalysis of intumescent flame retardancy of polypropylene by metallic compounds. *Polym Adv Technol.* 2003;14(1):3–11. doi:10.1002/pat.265.
13. Gallo E, Schartel B, Acierno D, Russo P. Flame retardant biocomposites: synergism between phosphinate and nanometric metal oxides. *Eur Polym J.* 2011;47(7):1390–401. doi:10.1016/j.eurpolymj.2011.04.001.
14. Gallo E, Braun U, Schartel B, Russo P, Acierno D. Halogen-free flame retarded poly(butylene terephthalate) (PBT) using metal oxides/PBT nanocomposites in combination with aluminium phosphinate. *Polym Degrad Stabil.* 2009;94(8):1245–53. doi:10.1016/j.polydegradstab.2009.04.014.
15. Dogan M, Bayramli E. The flame retardant effect of aluminum phosphinate in combination with zinc borate, borophosphate, and nanoclay in polyamide-6. *Fire Mater.* 2014;38(1):92–9. doi:10.1002/fam.2165.
16. Weil ED, Patel NG. Iron compounds in non-halogen flame-retardant polyamide systems. *Polym Degrad Stabil.* 2003;82(2):291–6. doi:10.1016/S0141-3910(03)00183-6.
17. Liu X, Zhou Y, Peng H, Hao JW. Catalyzing charring effect of solid acid boron phosphate on dipentaerythritol during the thermal degradation and combustion. *Polym Degrad Stabil.* 2015;119:242–50. doi:10.1016/j.polydegradstab.2015.05.020.
18. Zhou Y, Feng J, Peng H, Qu H, Hao J. Catalytic pyrolysis and flame retardancy of epoxy resins with solid acid boron phosphate. *Polym Degrad Stabil.* 2014;110:395–404. doi:10.1016/j.polydegradstab.2014.10.009.
19. Liu X, Hao J, Gaan S. Recent studies on the decomposition and strategies of smoke and toxicity suppression for polyurethane based materials. *RSC Adv.* 2016;6(78):74742–56. doi:10.1039/C6RA14345H.
20. Lyon RE, Walters RN. Pyrolysis combustion flow calorimetry. *J Anal Appl Pyrol.* 2004;71(1):27–46. doi:10.1016/S0165-2370(03)00096-2.
21. Liu X, Salmeia KA, Rentsch D, Hao J, Gaan S. Thermal decomposition and flammability of rigid PU foams containing some DOPO derivatives and other phosphorus compounds. *J Anal Appl Pyrol.* 2017;124:219–29. doi:10.1016/j.jaap.2017.02.003.
22. Shi YQ, Yu B, Zhou KQ, Yuen RKK, Gui Z, Hu Y, et al. Novel CuCo₂O₄/graphitic carbon nitride nanohybrids: highly effective catalysts for reducing CO generation and fire hazards of thermoplastic polyurethane nanocomposites. *J Hazard Mater.* 2015;293:87–96. doi:10.1016/j.jhazmat.2015.03.041.
23. Bashirzadeh R, Gharehbaghi A. An investigation on reactivity, mechanical and fire properties of Pu flexible foam. *J Cell Plast.* 2010;46(2):129–58. doi:10.1177/0021955x09350805.
24. Cheng HF, Liu QF, Liu J, Sun B, Kang YX, Frost RL. TG–MS–FTIR (evolved gas analysis) of kaolinite-urea intercalation complex. *J Therm Anal Calorim.* 2014;116(1):195–203. doi:10.1007/s10973-013-3383-x.
25. Bozi J, Mihalyi MR, Blazso M. Study on temperature dependence of catalytic thermal decomposition of polyamides and polyurethanes mixed with acidic zeolites. *J Anal Appl Pyrol.* 2013;101:103–10. doi:10.1016/j.jaap.2013.02.005.
26. Varone JC. Cyanide poisoning: how much of a threat. *Fire Eng.* 2006;159(9):61–70.
27. Xu QW, Zhai HM, Wang GJ. Mechanism of smoke suppression by melamine in rigid polyurethane foam. *Fire Mater.* 2015;39(3):271–82. doi:10.1002/fam.2249.
28. Tsai KC, Kuan CF, Chen CH, Kuan HC, Hsu SW, Lee FM, et al. Study on thermal degradation and flame retardant property of halogen-free polypropylene composites using XPS and cone calorimeter. *J Appl Polym Sci.* 2013;127(2):1084–91. doi:10.1002/app.37700.
29. Chuang FS. Analysis of thermal degradation of diacetylene-containing polyurethane copolymers. *Polym Degrad Stabil.* 2007;92(7):1393–407. doi:10.1016/j.polydegradstab.2007.02.020.